Infection Risk-Based Ventilation Effectiveness Assessment in Cruise Ship Common Spaces Using Tracer Gas Measurements

Alo Mikola[1,2], *Martin* Kiil[1*], *Karl-Villem* Võsa[1], and *Jarek* Kurnitski[1,2]

[1]Department of Civil Engineering and Architecture, Tallinn University of Technology, Tallinn, Estonia
[2]Department of Civil Engineering, Aalto University, Espoo, Finland

Abstract. Ventilation is one of the main engineering measures to control the airborne respiratory infection transmission in shared indoor spaces. This paper conducts infection risk assessment on a cruise ship employing CO_2 tracer gas constant injection methodology to measure ventilation effectiveness. The study encompassed various communal areas such as a restaurant, bar, nightclub, and canteen. CO_2 data loggers were employed to record concentrations at breathing level, with tracer gas source was positioned at different locations. In most cases extract air concentration was not possible to measure reliably because of typical air distribution arrangements in ships. Measured tracer gas volume flow and supply airflow rate were used to determine extract air concentration needed to calculate contaminant removal effectiveness. Point source ventilation effectiveness values were then derived from the concentration data. The outcomes of this investigation offer significant findings for the design of infection risk-oriented ventilation strategies in contemporary cruise ship environments.

1 Introduction

Large cruise ships, which can carry more than 3000 people, are becoming an increasingly popular form of travel [1]. At the same time, it has been studied that respiratory diseases are common infectious illnesses on cruise ships [2]. It is stated that 22.3% of ocean line cruise ships had at least one case of COVID-19 from January to October 2020 [3]. To avoid the risk of spreading diseases, especially in the context of the COVID-19 pandemic, the performance of ventilation and air conditioning systems in different types of ships, should be reviewed [4].

Heating, ventilation and air conditioning systems are used as a primary disease control measure in ships, but in case these systems are not used correctly, they may contribute to the transmission of airborne diseases as been seen for example on Diamond Princess Cruise Ship [5–7]. The study of the Diamond Princess Cruise Ship is one of the most unique COVID-19 transmission case which showed the air recirculation roll in the transmission of virus and also this study was one of the first evidence of coronavirus transmission by aerosols [6,7].

The most common ventilation solutions in cruise ships are mechanical natural ventilation, supply-exhaust ventilation and recirculation based mechanical supply-exhaust ventilation [4,8]. In case of recirculation based mechanical supply-exhaust ventilation, the air conditioning system is typically integrated with ventilation system and the heating and cooling demands are covered using a warmer or cooler supply air temperature, respectively. The roll of the recirculation system in the transmission of virus has been proven [6,7]. In general, the recirculation cannot be turned off because the system will no longer be able to ensure the efficient cooling or heating of the rooms, while they are designed for recirculation of 40–60% from total airflow [4]. That is the main reason why the guidelines to decrease the spread of the virus, point out that the increasing the airflow, using the high-efficiency filters and applying advanced operation strategies for air-conditioning systems, should be considered [9].

In various COVID-19 studies, the classical Wells Riley model is used for calculating the long-range airborne infection risk [10–12]. At the same time, this model is limited to fully and ideally air mixing in a single zone and consequently, the airborne infection risk could be under-or overestimated [12]. To consider ventilation effectiveness of an actual air distribution solution, a method is proposed by REHVA [13] and Kurnitski et al [14].

The main goal of this study is to assess ventilation effectiveness with point source (ε_b) in modern cruise ship common spaces. These values are averaged from point source ventilation effectiveness of measurement with source location j (ε_b^j). For calculating ε_b^j, local air quality indexes at the measurement point P ($\varepsilon_{P,i}$), which in turn are calculated from the CO_2 traces gas steady state concentrations, recorded in the conducted experiments. In conclusion, the ε_b values provide insight regarding air exchange rate and ventilation design. These ε_b values are proposed to use as a correction factor for dimensioning infection risk-based ventilation [13–15], presuming mixing ventilation.

* Corresponding author: martin.kiil@taltech.ee

2 Methods

This section provides overview of the main methods used in the study. The research methodology flow chart is presented in Figure 1. The studied rooms were carefully chosen with the ship managers. In order to be successful, the HVAC personnel ensured the correct design air flow rates and temperatures in the examined rooms. Information regarding measured cruise ship rooms (section 2.1), measuring equipment (section 2.2) and calculating ventilation effectiveness (section 2.3) is described below.

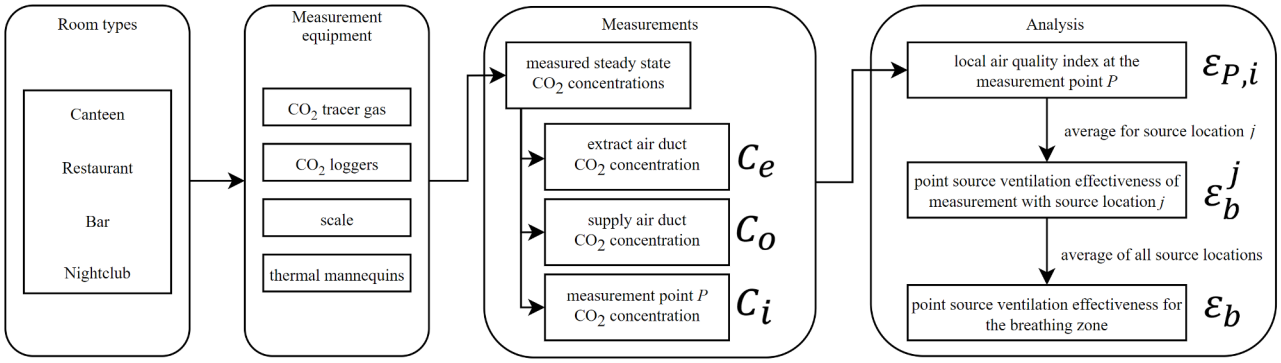

Figure 1. Flow chart of research methodology.

Studied cruise ship has mechanical balanced supply-exhaust ventilation system with heat recovery. For the fresh air supply, the air recirculation systems are not used. At the same time, to ensure the comfortable room temperatures, the separate air-based air conditioning systems are used in some of the rooms. The ventilation units that served the studied rooms were all equipped with rotary heat exchangers.

In cabins and some common rooms, there are two ventilation supply ducts system with one cold air duct and second warm air duct. If there is a cooling demand in cabin the supply air arrives from the cold duct and if there is a heating demand the air is supplied through the warm duct. In studied canteen, restaurant, bar and nightclub rooms, there is only one supply duct per room and if necessary, the air is reheated in duct-mounted water-based reheaters. In the studied rooms, the supply air was supplied through a perforated ceiling. Some supply valves were also used to compensate the local extract elements like kitchen hoods. The extract valves were generally located behind the perforated ceiling but every room there were also one to three extract valves that were installed to the same plane as the ceiling.

During the measurements the ventilation units worked in normal cruise mode. The setpoint of supply air temperature was as well in regular mode (about 18 degrees).

2.1 Cruise ship common spaces

The measurements were conducted in June 2023, in a modern cruise ship at Helsinki. The tests were carried out starting when the ship arrived at the port and ending before the ship departed. The experiments were executed out so that extraneous persons or other factors did not affect the steady state situation of CO_2 concentrations. The rooms used in the study are described in Table 1.

Table 1. Description of room cases for the ventilation effectiveness measurements.

Case	Image
Canteen A = 242 m² h = 2.5 m Q = 0.43 m³/s	
Restaurant A = 135.0 m² h = 3.1 m Q = 0.57 m³/s	
Bar A = 203.0 m² h = 3.1 m Q = 0.76 m³/s	
Nightclub A = 492.0 m² h = 4.5 m Q = 1.88 m³/s	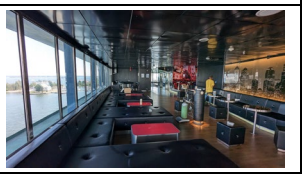

2.2 Measuring equipment

For ventilation effectiveness (ε_b) assessment traces gas experiments, carbon dioxide (CO2) is approved [16–20]. Data loggers were used to measure CO2 concentrations on the breathing plane (h = 1.1 m), in the supply air and in the extract air. The scale was used for gas dosing. The information of the measuring equipment is provided in Table 2 and Figure 2.

Table 2. Specifications of measuring equipment: CO_2 concentration logger [21] and gas mass weight scale [22].

	Onset HOBO MX1102A Data Logger	Kern FKB
Parameters	CO_2 concentration	weight
Range	0…5000 ppm	0.002…65 kg
Accuracy	±50 ppm + ±5 %	±0.001 kg
Image		

Thermal mannequins were used to imitate occupant heat gains. One of the mannequins was also used as a contaminant source, injecting tracer gas continuously to the room, connected with the CO_2 tank.

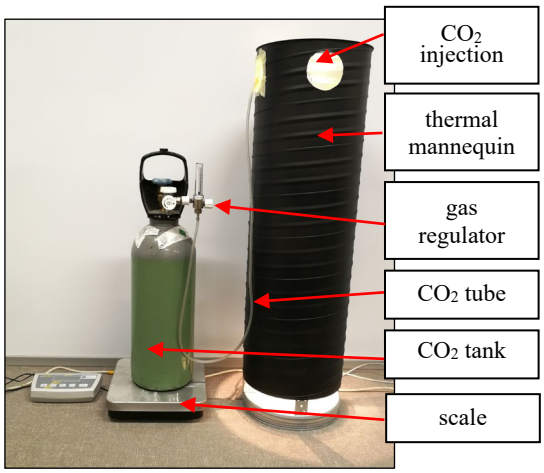

Figure 2. CO_2 tank connected with a thermal mannequin used as a contaminant source.

2.3 Calculating ventilation effectiveness

The ε_b signifies the capacity of a system to exchange air within a room or eliminate airborne contaminants [16]. To calculate ε_b, the average of values obtained from experiments conducted at different source locations (ε_b^j) is calculated. In the computation of ε_b^j (Equation 1), it is necessary to determine the average of local air quality index at different measurement points ($\varepsilon_{P,i}$). The calculation of $\varepsilon_{P,i}$ (Equation 2) relies on the steady-state concentrations at the measurement points ($C_{P,i}$). C_o represents supply air concentration and C_e refers to the concentration in the extract air duct. [13]

$$\varepsilon_b^j = \frac{1}{\frac{\sum_{i=1}^{k}\left(\frac{1}{\varepsilon_{P,i}}\right)}{k}} \quad (1)$$

$$\varepsilon_{P,i} = \frac{C_e - C_o}{C_{P,i} - C_o} \quad (2)$$

The Python programming language, utilizing the SciPy and Matplotlib software libraries, was employed for the result visualization.

3 Results and discussion

In canteen only one measurement was performed, in all other studied rooms two measurements were performed. In rooms where two measurements were conducted, one position of the contaminant source was close to the extract element, and another was as far as possible from the extract elements. In canteen the measurement point was was chosen so that it was sufficiently far from the position of the extraction valve.

The measurement results of room ventilation effectiveness vary from 0.60 to 0.97 (Table 3). It is possible to conclude that only in canteen the value of room ventilation effectiveness is close to the mixing ventilation ($\varepsilon_b = 1.0$). In other measured rooms, the room ventilation effectiveness is at a significantly lower level.

The measurement results of the local single ventilation effectiveness values ε_b^j vary from 0.50 to 0.97 (Table 3). The highest value was measured in canteen ($\varepsilon_b^j = 0.97$, Figure 7), which is close to the ideal mixing conditions. The lowest values were measured in nightclub ($\varepsilon_b^j = 0.50$) and in restaurant ($\varepsilon_b^j = 0.57$, Figure 6).

Table 3. Point source ventilation effectiveness with source location *j* and point source ventilation effectiveness for the breathing zone by room type and source positions.

Room	ε_b^j	ε_b
Canteen	0.97	0.97
Restaurant, source position 1	0.56	0.71
Restaurant, source position 2	0.87	
Bar, source position 1	0.64	0.70
Bar, source position 2	0.76	
Nightclub, source position 1	0.70	0.60
Nightclub, source position 2	0.50	

The net floor area per extract unit (Figure 3) ranges from 23 to 81 m^2 and distance to the nearest extract element (Figure 4) ranges from 2.5 to 4.5 m. There is no direct correlation between floor area and room ventilation effectiveness. Also, there is not significant correlation between the distance to the nearest extract element and values of $\varepsilon_{P,i}$. In the same way the value of the mean distance to the extraction points (Figure 5) does not cause significant change in the results.

It might be hypothesized that an increased number of ventilation extraction points and reduced distances to the elements could lead to improved ε_b^j and ε_b outcomes. At the same time, the measurement results of this study show that the position of extract elements has no significant effect to the values of room ventilation effectiveness. It can be generalized that measurement results indicate that this is not a rule of thumb and other ventilation design parameters need to be taken into account. Also, there were too few measurement points in this study to perform a competent statistical analysis of the correlation values.

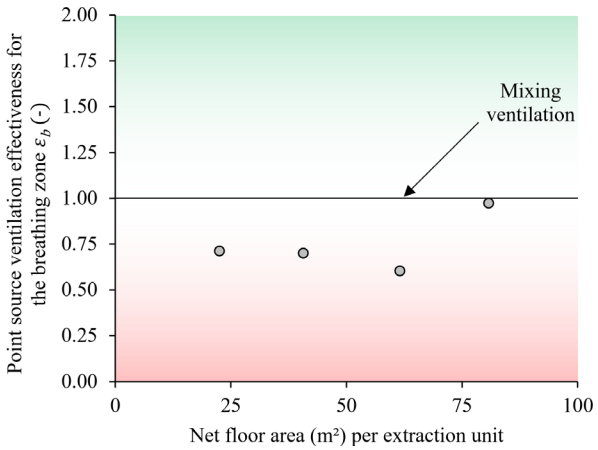

Figure 3. Point source ventilation effectiveness for the breathing zone results by net floor area per extraction unit.

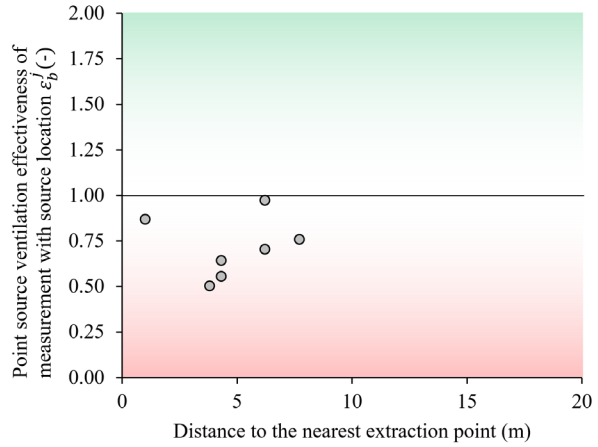

Figure 4. Point source ventilation effectiveness of measurement with source location *j* results by distance to the nearest extraction point.

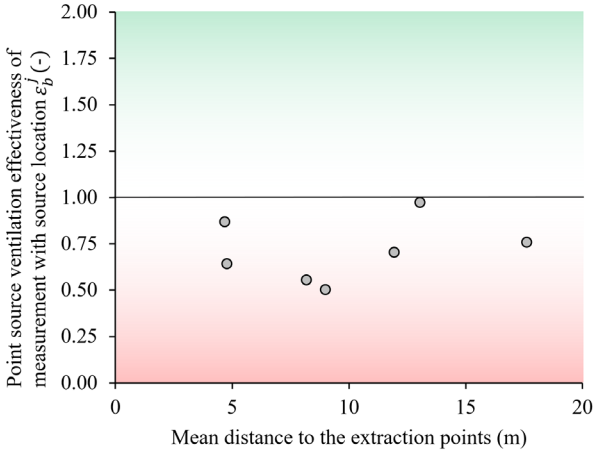

Figure 5. Point source ventilation effectiveness of measurement with source location *j* results by mean distance to the extraction points.

The ε_b^j results with the contaminant source location on the floor plan of canteen and restaurant with position 2 are visualized on Figure 6 and Figure 7. As it can be seen in Figure 6, there is a dividing wall between the two restaurant rooms. As the position 2 is located in the first larger space, the values of local air index are at a much higher level in the back room. This indicates that air mixing between two parts of the restaurant is limited which means that transmission of airborne diseases is also limited between these rooms.

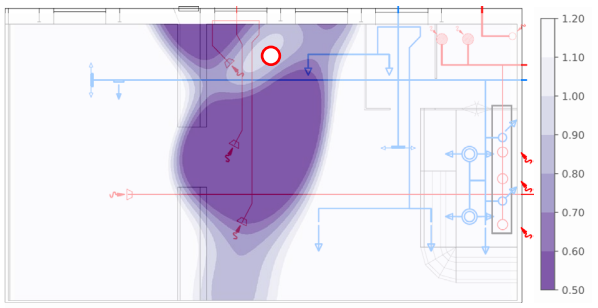

Figure 6. Local air quality index values in the restaurant.

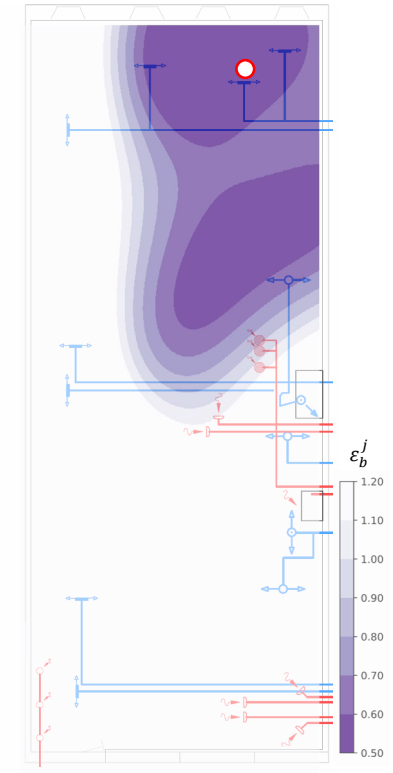

Figure 7. Local air quality index values in the canteen.

The main limitations of the study are the factors such as a generally larger floor area, partial openness, and variations in ventilation supply and extraction may significantly impact measuring accuracy of the ventilation effectiveness in these rooms. While the measurements with a point source highlight ventilation effectiveness considerably lower than in fully mixing there is good potential for air distribution solutions development to achieve better efficiency.

4 Conclusions

In this study, common cruise ship spaces such as canteen, restaurant, bar, and nightclub were examined to assess local air quality index and ventilation effectiveness with a point source using CO_2 tracer gas method. In conclusion, we found that:

- Three rooms out of examined four rooms did not meet the mixing ventilation criteria as measured ε_b ranged 0.6-0.7;
- The quantity or proximity to ventilation extraction points does not necessarily ensure higher ε_b or ε_b^j values;
- The spatial placement of a source of contaminants significantly influences the spread of pathogens;
- In the case of infection risk-based ventilation design involving a contaminant point source, ε_b values serve as an adjustment factor for the mixing ventilation airflow rate.

Acknowledgement

This work was supported by the Finnish Work Environment Fund project LAIVA (TSR 220253), by the Estonian Research Council grant (PRG2154), and by the Estonian Centre of Excellence in Energy Efficiency, ENER (grant TK230) funded by the Estonian Ministry of Education and Research. Nordic Ventilation Group and REHVA Technology and Research Committee COVID-19 Task Force are greatly acknowledged for support.

References

1. Wilson, M.E. The traveller and emerging infections: sentinel, courier, transmitter. *J. Appl. Microbiol.* **2003**, *94*, 1–11.
2. Zheng, L.; Chen, Q.; Xu, J.; Wu, F. Evaluation of intervention measures for respiratory disease transmission on cruise ships. *Indoor built Environ.* **2016**, *25*, 1267–1278.
3. Willebrand, K.S.; Pischel, L.; Malik, A.A.; Jenness, S.M.; Omer, S.B. A review of COVID-19 transmission dynamics and clinical outcomes on cruise ships worldwide, January to October 2020. *Eurosurveillance* **2022**, *27*, 2002113.
4. Mihai, V.; Rusu, L. An overview of the ship ventilation systems and measures to avoid the spread of diseases. *Inventions* **2021**, *6*, 55.
5. Correia, G.; Rodrigues, L.; Da Silva, M.G.; Gonçalves, T. Airborne route and bad use of ventilation systems as non-negligible factors in SARS-CoV-2 transmission. *Med. Hypotheses* **2020**, *141*, 109781.
6. Almilaji, O. Air recirculation role in the spread of COVID-19 onboard the diamond princess cruise ship during a quarantine period. *Aerosol Air Qual. Res.* **2021**, *21*, 200495.
7. Almilaji, O.; Thomas, P.W. Air recirculation role in the infection with COVID-19, lessons learned from Diamond Princess cruise ship. *medRxiv* **2020**, 2007–2020.
8. Brækken, A.; Gabrielii, C.; Nord, N. Energy use and energy efficiency in cruise ship hotel systems in a Nordic climate. *Energy Convers. Manag.* **2023**, *288*, 117121.
9. Xia, Z.; Guan, H.; Qi, Z.; Xu, P. Multi-Zone Infection Risk Assessment Model of Airborne Virus Transmission on a Cruise Ship Using CONTAM. *Buildings* **2023**, *13*, 2350.
10. Sun, C.; Zhai, Z. The efficacy of social distance and ventilation effectiveness in preventing COVID-19 transmission. *Sustain. cities Soc.* **2020**, *62*, 102390.
11. Guo, Y.; Qian, H.; Sun, Z.; Cao, J.; Liu, F.; Luo, X.; Ling, R.; Weschler, L.B.; Mo, J.; Zhang, Y. Assessing and controlling infection risk with Wells-Riley model and spatial flow impact factor (SFIF). *Sustain. Cities Soc.* **2021**, *67*, 102719.
12. Aganovic, A.; Cao, G.; Kurnitski, J.; Wargocki, P. New dose-response model and SARS-CoV-2 quanta emission rates for calculating the long-range airborne infection risk. *Build. Environ.* **2023**, *228*, 109924.
13. Rehva Health-based target ventilation rates and design method for reducing exposure to airborne respiratory infectious diseases. REHVA proposal for post-COVID target ventilation rates. *Rehva* 2023.
14. Kurnitski, J.; Kiil, M.; Mikola, A.; Vosa, K.-V.; Aganovic, A.; Schild, P.; Seppänen, O. Post-COVID ventilation design: Infection risk-based target ventilation rates and point source ventilation effectiveness. *Energy Build.* **2023**, *296*, 113386.
15. Kurnitski, J.; Kiil, M.; Wargocki, P.; Boerstra, A.; Seppänen, O.; Olesen, B.; Morawska, L. Respiratory infection risk-based ventilation design method. *Build. Environ.* **2021**, *206*, 108387.
16. Mundt, M.; Mathisen, H.M.; Moser, M.; Nielsen, P. V Ventilation effectiveness: Rehva guidebooks. **2004**.
17. Batterman, S. Review and extension of CO2-based methods to determine ventilation rates with application to school classrooms. *Int. J. Environ. Res. Public Health* **2017**, *14*, 145.
18. Chung, K.-C.; Hsu, S.-P. Effect of ventilation pattern on room air and contaminant distribution. *Build. Environ.* **2001**, *36*, 989–998.
19. ISO/TC 163; CEN/TC 89 ISO 12569:2017 Thermal performance of buidlings and materials. *Determ. Specif. airflow rate Build. - Tracer gas dilution method* **2017**.
20. ISO/TC 146 ISO 16000-8:2007 Indoor air - Part 8: *Determ. local mean ages air Build. Charact. Vent. Cond.* **2007**.
21. Onset Computer Corporation HOBO MX1102A data logger Available online: https://www.onsetcomp.com/products/data-loggers/mx1102a/.
22. KERN & SOHN GmbH Kern FKB datasheet Available online: https://www.kern-sohn.com/en/FKB.